

1 Soil Frost Controls Streamflow Generation Processes in
2 Headwater Catchments

3 Jones, Mariel W. ^{1,2}, Sebestyen, Stephen D. ³, Dymond, Salli F. ⁴, Ng, G.H.
4 Crystal ^{2,5}, Feng, Xue ^{1,2}

5 ¹Department of Civil, Environmental, and Geo- Engineering, University of Minnesota, Twin Cities,
6 Minneapolis, MN, USA

7 ²Saint Anthony Falls Laboratory, University of Minnesota, Twin Cities, Minneapolis, MN, USA
8 ³Northern Research Station, USDA Forest Service, St. Paul, MN, USA

9 ⁴Department of Earth and Environmental Sciences, University of Minnesota, Duluth, Duluth, MN, USA

10 ⁵Department of Earth and Environmental Sciences, University of Minnesota, Twin Cities, Minneapolis,
11 MN, USA

12 Key Points:

- 13 • Long-term data at two northern peatland-dominated catchments show that de-**
14 crease in annual streamflow is not correlated with climatic drivers.
- 15 • Spring streamflow is controlled by hydrologic connectivity across the landscape,**
16 from snowpack to surface water storage to streams.
- 17 • Soil frost, when present, is a key explanatory variable in determining the timing**
18 and magnitude of spring streamflow.

Corresponding author: M. W. Jones, jone3247@umn.edu

Corresponding author: X. Feng, feng@umn.edu

19 **Abstract**

20 The relationship between snowmelt and spring streamflow is changing under warming
21 temperatures and diminishing snowpack. At the same time, the hydrologic connectivity
22 across catchment landscape elements, such as snowpack and surface wetlands, can
23 play a critical role in controlling the routing of snowmelt to streams. The role of hydro-
24 logic connectivity is important in headwater regions of the continental northern latitudes,
25 where catchments have low topographic relief and seasonally frozen ground. Neverthe-
26 less, the effects of soil frost on the sequence, timing, and magnitudes of hydrologic events
27 that drive the movement of water from a snowpack to a stream are not fully understood.
28 Therefore, we examine two questions: first, what is the flowpath that snow melt and pre-
29 cipitation from spring rain events takes to generate spring streamflow, and second, what
30 hydrologic, climatic, or landscape variables exert the most control on the magnitude of
31 streamflow? Here, we use long-term hydrological records from the two reference basins
32 at the Marcell Experimental Forest in northern Minnesota to analyze the cascading ef-
33 fects across precipitation, snow, water table elevation, soil frost, and streamflow in peatland-
34 dominated headwater catchments. We identify a sequence of fill-and-spill effects across
35 the landscape that control the timing of spring streamflow generation. Then, we use step-
36 wise regression to show that soil frost is a key supporting predictor for both the mag-
37 nitude of streamflow in the spring as it adds significantly to the predictive power of pre-
38 cipitation and water table elevation. Our results highlight the importance of recogniz-
39 ing the role of soil frost, when present, on the partitioning of snowmelt between over-
40 land runoff and water table recharge during the critical snowmelt period, as well as the
41 later partitioning between evapotranspiration and subsurface flows.

42 **1 Introduction**

43 In snow-dominated, seasonally-frozen catchments, spring streamflow timing and mag-
44 nitude have been affected by a warming winter climate. For instance, estimates have shown
45 that, over the last century, spring streamflow peaks have shifted earlier by 4.5 to 8.6 days
46 in the northern hemisphere (Hodgkins & Dudley, 2006) and 8.7 to 14.3 days in the north-
47 central United States (Ryberg et al., 2016). These shifts in streamflow responses par-
48 tially result from decreases in snow pack size (Ford et al., 2020), including shifts in pre-
49 cipitation from snow to rain. Decreasing snowfall fraction, or the portion of precipita-

50 tion falling in the form of snow, within a single catchment has been shown to lead to earlier
51 spring streamflow peaks (Barnett et al., 2005), as well as decreases in mean annual
52 streamflow (Berghuijs et al., 2014; Foster et al., 2016).

53 However, the influence of snow fraction on streamflow can be complicated by the direct
54 effects of warming air temperature on the rate of snowmelt. Faster snowmelt rates, which
55 can occur when spring warming arrives earlier, have been shown to lead to larger spring
56 streamflow peaks and increased runoff and flood risk (Trujillo & Molotch, 2014). At the
57 same time, warming temperatures can also increase surface energy and evapotranspiration
58 later in the spring, which can have a counteracting effect that decreases streamflow
59 (Badger et al., 2021). Even so, the relative importance of snow fraction versus temperature-
60 driven land surface evaporative loss on streamflow remains unclear, with studies showing
61 that either could serve as a dominant driver of streamflow in different future climate
62 scenarios (Foster et al., 2016). Therefore, the complex interactions among climate, snow,
63 and hydrological processes as the spring progresses remains an open research question.

64 The climatic effects on streamflow are mediated by the hydrologic connectivity on the
65 landscape, which is controlled by a range of surface and subsurface storage components
66 that accelerate or inhibit the flow pathways connecting water as precipitation inputs to
67 streamflow (Pringle, 2003). For instance, snow-water equivalent (SWE), the total amount
68 of water stored in a snowpack, represents a temporary storage of precipitation in a frozen
69 state on the land surface, until it is released during the spring as snowmelt. This storage
70 behavior temporarily “halts” the flow of water until it becomes available in liquid
71 form again (Musselman et al., 2021). As such, the timing of snow disappearance and the
72 duration of snowmelt period exhibit strong influence on snowmelt runoff, streamflow peaks,
73 and overall water availability in the spring. The relationships between snowmelt and stream-
74 flow are commonly studied in sites monitored using the SNOTEL network in the west-
75 ern United States (Leuthold et al., 2021; Heldmyer et al., 2021; Trujillo & Molotch, 2014),
76 where, due to the well-defined surface topography and bedrock geology in mountainous
77 regions, the flow path from snowmelt to streamflow is fairly direct (Schneider & Molotch,
78 2016). Surface wetlands represents another storage for precipitation. Surface wetlands
79 may occur in areas of low topographic relief, and water within wetlands is stored until
80 the water table elevation (WTE) increases over a threshold elevation, causing overland
81 flow or lateral flow out of the wetland. The WTE to streamflow relationship is often the
82 focus in studies on geographically isolated wetlands, which demonstrate clear connec-

83 tivity among precipitation, WTE, and surface runoff (Cohen et al., 2016; Golden et al.,
84 2016; Verry et al., 2011). In geographically isolated wetlands, the WTE is the most im-
85 portant predictor of landscape connectivity because it determines the level of isolation
86 between the wetland and its surrounding surface water bodies (Winter & LaBaugh, 2003).

87 As the height of the water table rises above the wetland surface levels, the excess wa-
88 ter flows over the landscape to a surrounding stream, demonstrating the ‘fill-and-spill’
89 flow dynamics characteristic of hydrologic storage mechanisms (Cohen et al., 2016; Win-
90 ter & LaBaugh, 2003; McDonnell et al., 2021; Leibowitz & Vining, 2003).

91 Despite the importance of snowpack and wetlands in determining the connectivity to and
92 therefore timing and magnitude of streamflow, these near-surface storage components
93 have rarely been studied together, especially in conjunction with another important land-
94 scape driver: soil frost. In areas of seasonally frozen ground, air temperature, snow, and
95 soil moisture content control frost depths, which influence the snowmelt partitioning be-
96 tween overland flow and subsurface recharge (Aygün et al., 2019; Verry et al., 2011). Frozen
97 ground restricts the infiltration of snowmelt and water table recharge, thereby increas-
98 ing surface runoff (Zhao & Gray, 1999; Kane & Stein, 1983). The combined effects of
99 rising winter temperatures and shrinking snowpack will also reduce the frost layer, re-
100 sulting in an overall increase in the rate of groundwater recharge due to earlier snow melt
101 and higher infiltration rates (Jyrkama & Sykes, 2007). The importance of frost is depen-
102 dent on a diverse range of factors, some of which are difficult to predict or remain un-
103 certain; while frost is more likely to affect streamflow in small catchments, cold climates
104 and forested land cover can limit the effects frost has on streamflow (Ala-Aho et al., 2021).

105 For example, a soil frost model developed using data from a catchment in northern Swe-
106 den showed no clear effect of soil frost on either the timing or magnitude of streamflow
107 runoff. This lack of connection between frost and streamflow was likely due to limited
108 frost occurrence (frost formed in only slightly more than half the years) or because the
109 frost often had thawed before spring melt and streamflow onset (Lindström et al., 2002).
110 In contrast, at a site in southern Switzerland, only 25-35% of the melt water infiltrated
111 into the soil in a winter with thin snowpack and thick frost layer, compared to 90-100%
112 in a different winter that had a deep snowpack and thin frost layer (Bayard et al., 2005).

113 As the effect of frost is variable across catchments and its presence can greatly affect spring
114 runoff, it is important to consider that, first, soil frost can be quite heterogeneous across
115 the landscape, a variability that is not captured in soil profile studies (Zhao & Gray, 1999;

116 Kane & Stein, 1983). Second, soil frost varies from year to year, depending on winter
117 climate and precipitation. Capturing these spatial and temporal variations is key to better
118 understanding the relationship between soil frost and streamflow generation. In this
119 study, we use long-term climatological and hydrological data to show a clear cascade of
120 hydrological connectivity throughout the landscape and to determine the relative strengths
121 of climatic and land surface variable in predicting annual streamflow trends.

122 Peatlands provide an ideal environment in which to study interacting surface and sub-
123 surface flows in the spring snowmelt season. The majority of peatlands are located in
124 northern latitudes, where seasonal soil frost is becoming more dynamic under climate
125 change, as soils transition from permanently frozen to seasonally frozen soils (Bridgman
126 et al., 2013). Additionally, wetlands, including peatlands, are the single largest natural
127 source of methane, contributing about a third of total global emissions (Gorham, 1991),
128 with methane emissions from peatlands strongly controlled by seasonal water table dy-
129 namics and snowmelt dynamics (Feng et al., 2020). Therefore, it is critical to understand
130 how the increasingly dynamic frost conditions will impact wetland water table, and by
131 consequence, the role that peatlands play in both global and regional methane budgets.
132 Regionally, headwater streams and wetlands provide innumerable ecosystem services, in-
133 cluding regulating streamflow responses and improving downstream water quality (Colvin
134 et al., 2019; Alexander et al., 2007). This critical hydrological landscape provides the ideal
135 location to examine the effects of shifting spring hydrologic cascades on the wider net-
136 work of low-relief catchments.

137 We focus on relationships among climate, hydrology, and landscape elements by exam-
138 ining two questions related to hydrologic connectivity in snow-dominated, low-relief peat-
139 land catchments: how do snow, frost, and surface wetlands mediate the flow paths from
140 precipitation to spring streamflow? And what hydrologic, climatic, or landscape vari-
141 ables most control the magnitude of streamflow? As the effect of frost is variable across
142 catchments and its presence can greatly affect spring runoff, it is important to consider
143 that, first, soil frost can be quite heterogeneous across the landscape, a variability that
144 is not captured in soil profile studies (Zhao & Gray, 1999; Kane & Stein, 1983). Second,
145 soil frost varies from year to year, depending on winter climate and precipitation. In this
146 study, we will examine these questions in two peatland catchments at the Marcell Ex-
147 perimental Forest (MEF) in northern Minnesota (USA), using statistical approaches ap-
148 plied to the analysis of long-term datasets. By focusing on two watersheds with long data

records, we contribute new findings to both unresolved complexities of the importance of soil frost in forested catchments and expand upon existing soil profile, event-scale, and modeling soil frost studies. We first parameterize the processes that occur in the spring season by extracting key hydrological events from the long-term time series and analyze the timing across each of these events through ranking. Then, we use stepwise regression to identify the importance of winter and spring season variables for predicting annual streamflow. Together, answers to these questions will illustrate the importance of considering soil frost in headwater catchments.

2 Methodology

2.1 Site Description

Our catchments are located within the USDA Forest Service Marcell Experimental Forest (MEF, Lat. 47:31:52N, Long. 93:28:07W) near Grand Rapids, Minnesota (USA). The MEF sits on the climatic transition region between areas of seasonally frozen ground and northern boreal regions, and has six peatland dominated catchments that have been under long term observation since 1961 (Sebestyen et al., 2011). The S2 and S5 research catchments are reference basins with central peatlands surrounded by upland forests on mineral soils. Records for these sites include hydrologic, meteorological, and water chemistry data (Sebestyen, Lany, et al., 2021). Minnesota climate is strongly continental with warm, humid summers and cold, dry winters. From 1961 to 2019, mean annual temperature at the catchments was 3.5 °C (Sebestyen, Lany, et al., 2021). Average annual temperature has been increasing by 0.4 °C per decade since 1961 with the majority of the warming occurring over the winter months (Sebestyen et al., 2011, January to March, 0.7 °C per decade). Annual precipitation averages 79 cm, with one third of precipitation falling in the form of snow (Sebestyen, Lany, et al., 2021). Snow cover in the peatland starts in late October and November and usually lasts until March or April of the following year. There has been no change over time in maximum snow water equivalent under coniferous and open areas but significant decline under deciduous covers (Sebestyen et al., 2011).

177 **2.1.1 South Unit - S2 Bog**

178 The S2 watershed has a total size of 9.7 ha which is made up of a 3.2 ha domed peat-
 179 land encircled by upland forests. The upland vegetation is dominated by aspen (*Pop-*
 180 *ulus tremuloides*, *Populus grandidentata*) stands. The peatland is covered by black spruce
 181 *Picea mariana* and *Sphagnum* mosses. The bog topography is characterized by a slightly
 182 domed peat surface rising 18 cm at its peak with a presumed parallel peatland water ta-
 183 ble. There is a streamflow outlet elevation of 420 m above sea level (Richardson et al.,
 184 2010). Measurements of the peatland WTE are taken near the highest elevation of the
 185 bog using a stripchart recorder and daily maximum water table is recorded (Sebestyen
 186 et al., 2011). Streamstage is measured using a V-notch weir and strip chart recorder at
 187 the South-west end of the catchment (Verry et al., 2018, for data and metadata). Win-
 188 ter snow and frost depth were measured biweekly from 1962 to 2021 starting in Febru-
 189 ary and continuing through snow disappearance (Sebestyen, Burdick, et al., 2021, for data
 190 and metadata). In S2 snow and frost measurements were taken biweekly on two upland
 191 snow courses in aspen stands and one bog snow course in a black spruce stand.

192 **2.1.2 North Unit - S5 Bog**

193 S5 is a larger peatland on the North Unit of the Marcell Experimental Forest that is 52.6
 194 ha in size and contains five small satellite peatlands that drain into a central peatland
 195 that is 6.1 ha. The S5 uplands are have some older growth and more diverse with species
 196 of aspen, white cedar (*Thuja occidentalis*), white spruce (*Picea glauca*), balsam fir (*Abies*
 197 *balsamea*), pine (*Pinus strobus*, *Pinus resinosa*, *Pinus banksiana*), and mixed hardwoods
 198 with an average stand age of 100 years. Bog water table elevations are measured in a
 199 similar way as in S2 using stripchart recorders to monitor a central peatland well. Stream-
 200 stage is measured using a V-notch weir at the Northeast corner of the watershed. Sim-
 201 ilar to the S2 watershed, snow depth, SWE, and frost depth measurements are taken bi-
 202 weekly in S5 beginning in February and continue through snow disappearance. There
 203 are four snow courses in S5, one in an upland clearing with the S5 meteorological sta-
 204 tion, one in the bog, and two in the uplands (Sebestyen et al., 2011; Sebestyen, Lany,
 205 et al., 2021).

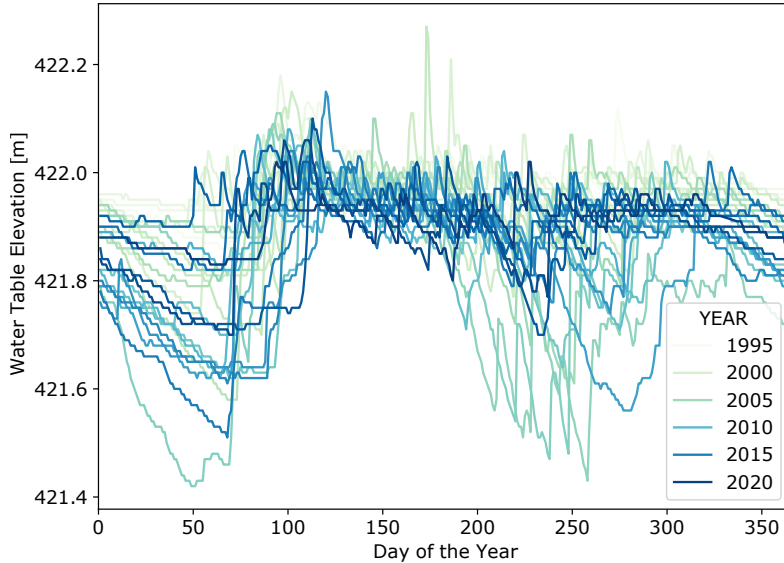


Figure 1. Daily water table elevation in the S2 bog. Annual water table time series colored by year from 1995 (light green) to 2020 (dark blue).

206

2.1.3 Forestry Sciences Laboratory, Grand Rapids, MN

207

To increase the temporal resolution and coverage of the snow course data from the MEF, we used supplemental data with a longer record from the USDA Forest Service Grand Rapids Forestry Sciences Laboratory (Lat. 47:14:9.2N, Long. 93:31:41.9W), approximately 48 km south of the MEF. Here precipitation, snow inputs, and snow depth are all taken daily from 1915 (precipitation) and 1948 (snow inputs, depth) onwards. A correlation between precipitation inputs at the two sites is shown in Figure S1. In Grand Rapids the mean annual temperature from 1950 to 2020 was 4.5°C and precipitation was 71 cm. Snow depth data from 1974-1989 were missing most of the daily values and so these years were removed from the analysis.

216

2.2 Characterizing the timing and magnitude of hydrological events

217

We first identified hydrological events in the winter and spring periods and derived metrics characterizing two key aspects of these events: magnitude and timing in the water year (defined here as October 1st to September 30th). These standardized metrics can be used to compare hydrological events across multiple years (1995-2020) and detect trends over time. We focused on the winter to spring seasonal transition, because this transi-

222 tion is a period of high flow that often contributes the most to the annual streamflow
223 yield.

224 The metrics for the snowpack dataset were calculated based on the triangle method used
225 by Trujillo and Molotch (2014) for SWE data. The method, which was developed to iden-
226 tify key snow appearance, disappearance, and peak values for snowpacks in the western
227 United States, has not been applied to snow depth data in Minnesota before. However,
228 annual snow depth time series from Grand Rapids demonstrate a similar triangle struc-
229 ture, so we anticipate that the method will be effective for our needs. Here, we applied
230 the triangle method to the Grand Rapids snow depth data to derive snowpack metrics
231 for both the S2 and S5 catchments. The MEF snowpack data were not used for these
232 metrics because the biweekly data did not have high enough temporal resolution. Im-
233 plementing this method involved identifying three key dates in the snow season: the date
234 of snow appearance (DOA), the date of peak snow depth (DOP), and the date of snow
235 disappearance (DOD). The DOA and DOD values for each water year were determined
236 to be the first and last non-zero value of snow depth (with a seven-day buffer to control
237 any erratic early or late season snow events). To determine the DOP that best approx-
238 imates the transition between snow accumulation and ablation, it was necessary to iden-
239 tify first all potential peaks and then investigate the fit to a triangular function for snow
240 depth evolution. To do so, the *find_peaks* function from the *scipy.signal* package in Python
241 3.8 (Virtanen et al., 2020) was used to first identify all potential peak values between
242 the timing of the 10th and 90th percentile of snow accumulation (to ensure the detected
243 snowpack peak occurred near the middle of the snow season) which had snow depths above
244 half the annual mean. Then, each of the potential peaks was used to simulate snow depth
245 using a triangular function, where snow depth increases linearly from DOA to the date
246 of potential peak, then decreases linearly until it reaches zero at DOD. Each of these fits
247 (with its corresponding DOP) was then compared to the measured snow depth data us-
248 ing a nonparametric Mann-Kendall test for monotonic trends. The DOP whose corre-
249 sponding fit resulted in the highest correlation coefficient against measured snow depth
250 was selected for that year. The snow depth at DOP was also identified, as well as the
251 duration and rates of the accumulation and melt periods.

252 For the WTE metrics, we observed that the spring recharge period begins with a typ-
253 ically annual low value right before the spring climb to a seasonal high (Figure 1). For
254 measuring the magnitude of the spring climb, the overall duration of the recharge pe-

255 riod and total WTE recharge of the season were also identified. The *find_peaks* function
 256 was again used to select possible dates for the seasonal WTE trough and peak during
 257 the spring recharge period. For each of the several possible trough/peak pairs identified,
 258 the Mann-Kendall test was again used to compare a linear function of WTE recharge
 259 generated against the measured data. The pair with the highest correlation was selected
 260 for the timing metrics and their WTE values were recorded.

261 The spring streamflow timing metrics were selected as the maximum value of the first
 262 major peak of the spring season and the timing of first nonzero value as the onset of spring
 263 streamflow. The magnitude of the first spring streamflow peak was also recorded. Due
 264 to the limited resolution (i.e., biweekly) frost data from the MEF sites, we only identi-
 265 fied the maximum frost depth value and date of maximum.

266 2.3 Rank and Correlational Analysis

267 Each timing metric across the data record was examined for annual trends using linear
 268 regression across each water year (October 1st – September 30th). This analysis included
 269 examining six timing metrics to quantify spring seasonal hydrology: the peak snow depth
 270 (S_{peak}), the date of snow disappearance (S_{DOD}), the date of WTE trough (W_{trough}),
 271 the date of WTE peak (W_{peak}), the date of streamflow onset (Q_{onset}), and the date of
 272 the first streamflow peak (Q_{peak}).

273 A correlation analysis was used to examine the relationships between the timings of each
 274 of the same six variables of interest. For each year, the day of the water year in which
 275 these events occurred was recorded in a list and used to rank each of the variables (e.g.,
 276 if the maximum WTE occurred first among the six events in water year 2012, then it
 277 was given rank 1). The ranks for each event were then averaged across all years.

278 2.4 Multivariate Regression

279 We used multiple regression to examine the interactions among hydrological and clima-
 280 tological variables in controlling streamflow generation in the spring and throughout the
 281 year. A stepwise multiple regression model was built to predict the magnitude of total
 282 annual streamflow from a set of site-dependent and shared precipitation variables. A to-
 283 tal of six predictor variables were used: air temperature ($X_{AvgTemp}$), snowpack depth
 284 ($X_{SnowPeak}$), max annual frost thickness (X_{MFT}), average annual WTE (X_{WTE}), to-

Table 1. Magnitude variables used in the regression model

Variable	Description	Units
Y_{Flow}	Total annual streamflow, normalized by area	m
$X_{SnowPeak}$	Depth of the snow pack at its peak	cm
X_{MFT}	Maximum thickness of frost	cm
X_{WTE}	Annual average water table elevation	m
$I_{Watershed}$	Watershed, 0 for S2, 1 for S5	-
$X_{AvgTemp}$	Average annual temperature	°C
$X_{TotPrecip}$	Total annual precipitation	cm

285 tal annual precipitation ($X_{TotPrecip}$), and an indicator to designate either the S2 or S5
 286 watershed ($I_{Watershed}$) (Table 1). All data used in this model is site-specific. A random
 287 sampling of 60% of the years (1995-2020) were used for the stepwise analysis. This sub-
 288 set was then used to build sub-multiple regression models using different combinations
 289 of the predictor variables using a stepwise analysis. Each model tested was a subset of
 290 the full model, which contains all the predictor variables and all potential combinations
 291 of interaction terms. Here $\mathcal{P}()$ is the power set, or all combinations of the interaction term.

$$292 \quad Y_{Flow} \sim \beta_0 + \mathcal{P}(\beta_{i,j,k,l} X_{i,SnowPeak} X_{j,MFT} X_{k,WTE} I_{l,Watershed}) + \beta_2 X_{AvgTemp} + \beta_3 X_{TotPrecip} \quad (1)$$

293 A total of 668 sub-models were constructed from the full model shown in Equation (1).
 294 For each model, a second-order bias-corrected Akaike's Information Criterion (AICc) was
 295 used to compare predictive capacity, and the models with lower AICc ($\Delta AICc < 2$) were
 296 taken as 'candidate' models (Burnham et al., 2011). $\Delta AICc$ is the difference between
 297 the AICc value of the best fit model and the model of interest. A model with a similar
 298 goodness of fit to the best fit model will have a minimized $\Delta AICc$. Each candidate model
 299 was then used to predict the remaining 40% of the data set and validated for linearity,
 300 constant variance, and normality. In addition, each model was given a weight, W_i , which
 301 is the probability of the model given the data (Burnham et al., 2011). W_i is computed
 302 as the likelihood of a given model over the total number of models and can be read as
 303 "the probability of model i is w_i ". For each predictor variable, these weights were summed
 304 across the sub-models containing that particular predictor variable to obtain the over-
 305 all relative importance of each variable. This process was then repeated 1000 times with
 306 a different random sampling of years for each candidate model to determine an expected

307 range of RMSE. This processes was repeated to predict the magnitude of the first spring
 308 streamflow peak, Q_{Peak} , which is outlined in the supplementary materials.

309 To further evaluate the results from the variable importance analysis, a separate dom-
 310 inance analysis was run to determine the independent effects of each predictor variable
 311 within the best fit model (Budescu, 1993; Murray & Conner, 2009). This method allows
 312 us to consider the amount of variation in the annual streamflow data that is explained
 313 by each individual predictor variable while removing any covariance between predictors.
 314 It determines the relative explanatory power of each variable *within* a single model. This
 315 dominance analysis is different then the step-wise regression model analysis which de-
 316 termines variable importance *between* models. The dominance analysis was run using
 317 all of the data, not only the 60% random sampling.

318 3 Results

319 Total annual streamflow, normalized by respective catchment areas, decreased in S2 at
 320 a rate of 1.9 cm per water year over 25 years ($p < 0.005$, 1995-2020) and in S5 at a rate
 321 of 2.9 cm per water year also over 25 years ($p < 0.05$, Figure 2a). The decrease in an-
 322 nual streamflow occurred despite no statistically significant changes in snowfall fraction
 323 ($p = 0.69$; Figure 2b), annual precipitation ($p = 0.331$), snowfall inputs ($p = 0.829$), or
 324 winter air temperature ($p = 0.47$; Figure 2c) and only a small increase in mean annual
 325 air temperature of 0.4 °C per decade ($p = 0.0005$, Sebestyen et al. (2011)). Furthermore,
 326 annual streamflow across multiple years shows no statistically significant correlation with
 327 mean annual air temperature ($p = 0.775$). However, average annual WTE in the S2 peat-
 328 land is decreasing at a rate of 4 cm/decade ($p = 0.002$) with the trough WTE decreas-
 329 ing at a slightly faster rate of 6.5 cm/decade ($p = 0.066$).

330 3.1 Streamflow Generation

331 Results from the signal processing of hydrological data showed a consistent sequence of
 332 events as water traveled from the snowpack through the landscape to generate stream-
 333 flow. Figure 3 shows the relationship between the streamflow and WTE in S2 and S5.
 334 First, there is a clear WTE threshold that dictates the initiation of streamflow in both
 335 S2 and S5 (Figure 3a-b), which demonstrates the surface water storage must first be "filled"
 336 before it "spills" into the stream. There is also a direct and statistically significant re-

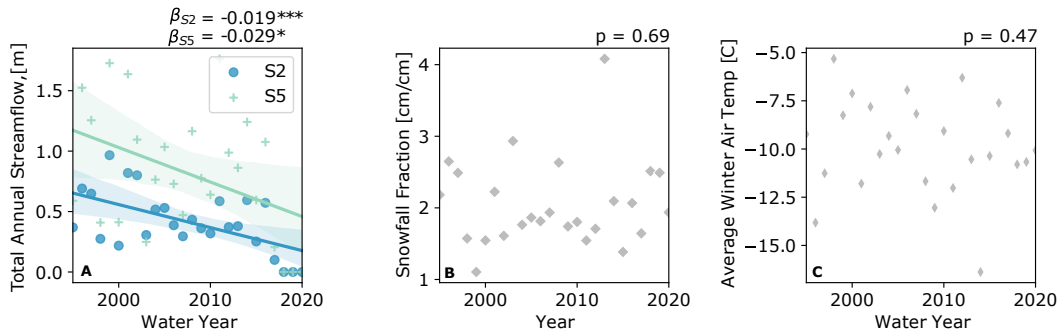


Figure 2. (A) Summary of decreasing annual streamflow trends in S2 and S5 at the MEF, (B) lack of snow or precipitation trends from the Grand Rapids meteorological station, and (C) lack of winter air temperature trends from the MEF meteorological station (Dec. 1st - March 31st). β values in (A) show the rate of water table change over time in S2 and S5. P-values show the insignificance of the annual trends in (B) and (C). Stars indicate the level of significance for each trend with *** denoting $p < 0.001$ and ** denoting $p < 0.05$. Shaded areas indicate a 95% confidence interval.

337 lationship between the timing of peak WTE and the first streamflow peak in both catch-
 338 ments across years (Figure 3c - d).

339 Figure 4 shows the ranked estimates for the timing of each hydrological event for 2013
 340 (top panel) and for all years of record (bottom panel). When averaged across years and
 341 catchments, dates of S_{peak} , W_{trough} , Q_{onset} , S_{DOD} , W_{peak} , and Q_{peak} occurred sequen-
 342 tially with mean dates of 135, 156, 166, 170, 187, and 190 respectively. Dates for WTE
 343 trough (W_{trough}) and peak (W_{peak}) were similar in S2 and S5, with S5 showing more vari-
 344 ation in trough dates and less variation in peak dates than S2. Streamflow onset (Q_{onset})
 345 in S5 typically occurred later than in S2 and with much higher temporal variation (mean
 346 164.7 and 168; SD of 14.8 and 21.7 respectively). Date of first streamflow peak (Q_{peak})
 347 was similar for both catchments, 190.4 and 190.1 respectively. While there is a clear se-
 348 quence of events during spring, the timing for most of the individual events is not cor-
 349 related (with the exception of Q_{peak} and W_{trough} as shown in Figure 3). For instance,
 350 the timing of peak snow, the timing of the WTE trough, and the timing of streamflow
 351 onset are not correlated (Figure S4).

352 3.2 Relative Impacts of Landscape Controls on Streamflow

353 The stepwise regression model (Equation 1) was used to determine the relative explana-
 354 tory power of each hydrological and climatological input variable on annual streamflow.

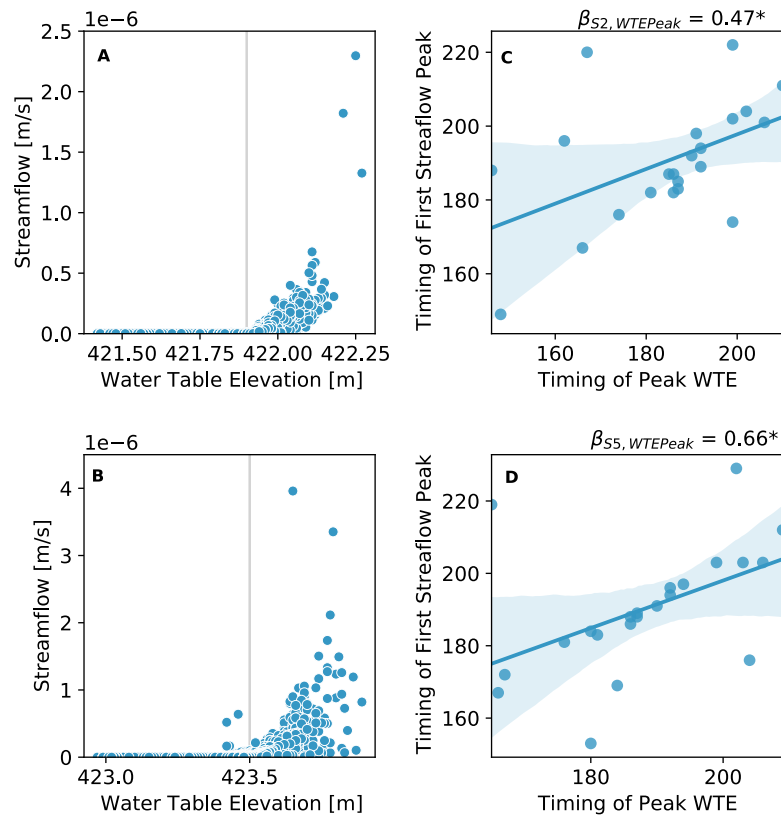


Figure 3. The non-linear relationship between water table elevation (WTE) and streamflow. (A - B) The thresholds for streamflow initiation in S2 and S5 respectively, shown at the daily time scale. (C-D) Show the relationship between the timing of peak WTE and the first detected streamflow peak in S2 and S5 respectively. β values are the slopes of the relationships in (C) and (D). The statistical significance of the relationships is shown using '*' to represent $p < 0.05$. Shaded areas indicate a 95% confidence interval.

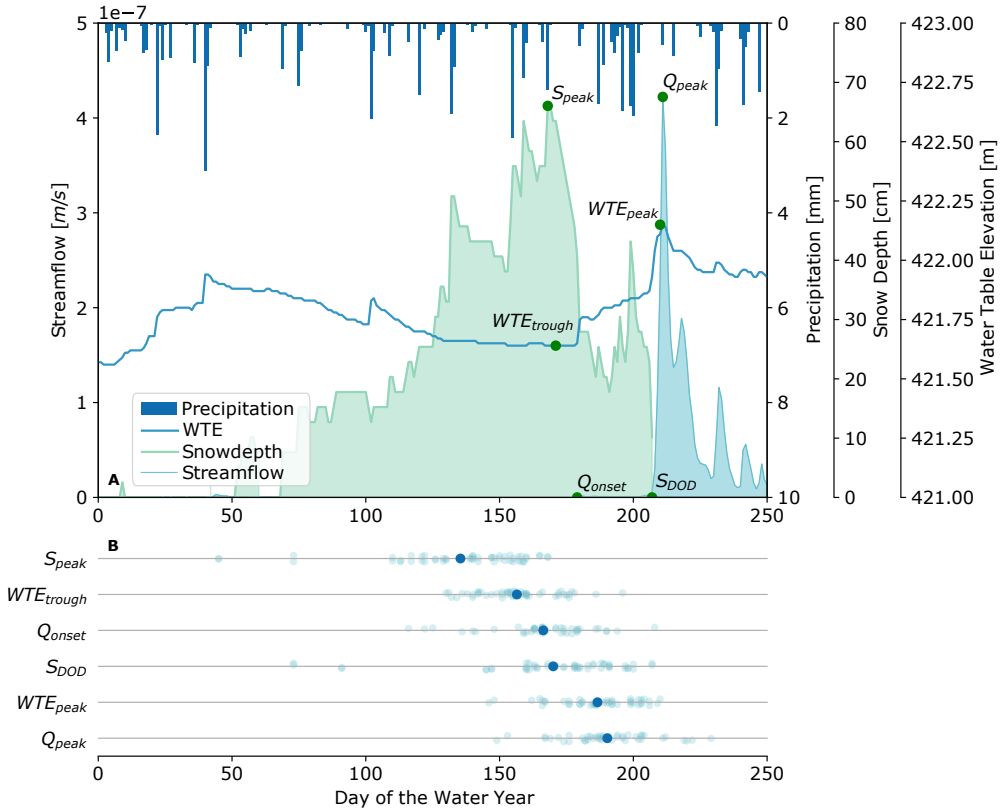


Figure 4. Hydrologic cascade from snowfall to streamflow. (A) A sample year, 2013, showing each data element overlaid with critical points derived using the parameterization methods. (B) Annual trends in the derived statistics for magnitude compiled over both catchments. Dark blue dots show the average date of occurrence for each metric over the time period from 1995-2020. The water year is defined as October 1st through September 31st of the following Gregorian calendar year.

355 Select model candidates (smallest values of Δ AICc) for predicting the total annual flow
 356 are shown in Table 2. The base model was ranked last of the 668 models with the high-
 357 est Δ AICc. Also listed are K, the degrees of freedom in the selected model, and w_i , or
 358 the probability of the model given the data. Of the metrics shown in Table 2, the value
 359 of w_i , or weight, is the most important as it shows the probability that of all of the mod-
 360 els considered, that model is the best model for making predictions.

361 Each model in Table 2 shows zero mean and standardized residuals, but all of the can-
 362 didate models also show a slight increasing trend in the variance as a function of the resid-
 363 uals, which may violate the constant variance assumption. The direction of the increase
 364 is not consistent. Using Cook's distance ($1 > \text{distance} > 0.5$), discharge in Model 3 for
 365 year 2013 and S2 was identified as an outlier (Cook, 2000). All other models show no
 366 outliers. The remaining validation years were then used to predict values of total annual
 367 flow and compare to the observed flows from the same year. Sample plots of these val-
 368 ues are shown in Figure 5.

369 Frost was an important predictor in the summed weights for each of the predictor vari-
 370 ables (Figure 5). The individual variables (top four rows) showed the highest importance,
 371 with maximum frost thickness being the most highly weighted variable with a weight of
 372 0.98 out of a possible normalized score of 1, meaning that frost had the most additive
 373 predictive power when present in a model. Mean frost thickness in S2 was 5.7 cm with
 374 a range of 0 to 36 cm (1995-2020). In S5, mean frost thickness is 10.5 cm with a range
 375 of 0 to 42 cm. The date of maximum frost at S5 occurred later in the season when com-
 376 pared to S2, and when ranked with other spring variables, occurred last. Total annual
 377 precipitation was ranked as the second most important predictor variable. However, when
 378 the dominance analysis is used on the top model, $Y_{Flow,1}$, only 12.3% of the total vari-
 379 ance explained by the model is explained by the maximum frost thickness. 49.4% of the
 380 total variance is explained by the water table elevation, 26% by precipitation, and 12.3%
 381 by the frost thickness and water table interaction term. When regression was also ap-
 382 plied to predict the magnitude at Q_{peak} , shown in Tables S1 and S2 of the supplemen-
 383 tary materials, snow depth was the most highly weighted variable (0.971) followed closely
 384 by maximum frost depth (0.923). Within the top weighted model, however, it was the
 385 snow depth and catchment interaction term that was describing the majority of the vari-
 386 ance (42.9%) followed by catchment (34.8%), maximum frost thickness (17.5%), and then
 387 snow depth (4.8 %). As a result, while frost may have a large weight when each model

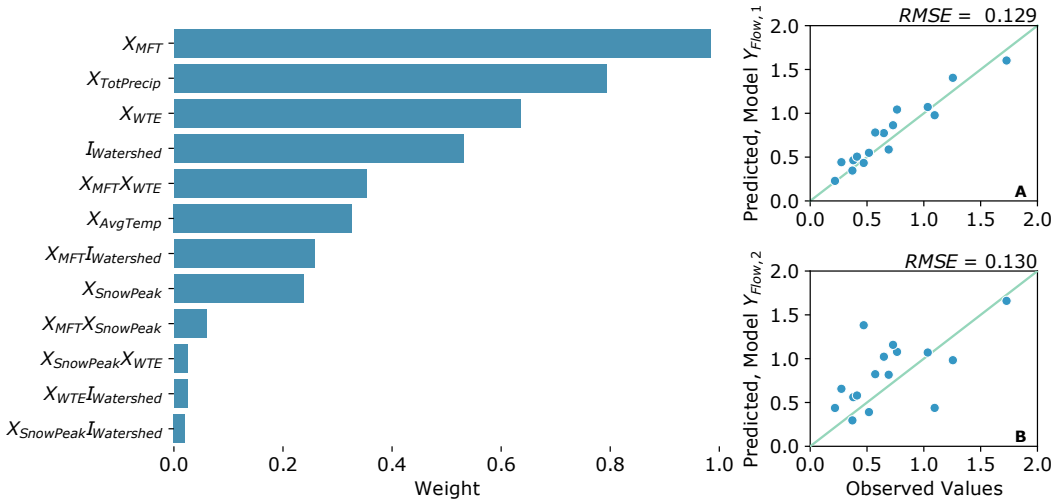


Figure 5. Model results showing: Left, variable importance from the stepwise regression model. Terms of order 3 or higher have been removed because of insignificance (summed weight = 0) (A-B) show a sample of two observed models from candidate model $Y_{Flow,1}$ and $Y_{Flow,2}$ with the minimum RMSE values from all 1000 iterations. Green line shows the one to one relationship.

Table 2. Selected Models for total annual streamflow in order of AICc

Model	K	AICc	Δ AICc	Weight
$Y_{Flow,1} \sim \beta_0 + \beta_1 X_{MFT} + \beta_2 X_{WTE} + \beta_3 X_{TotPrecip} + \beta_4 X_{MFT}X_{WTE}$	6	5.13	0	0.16
$Y_{Flow,2} \sim \beta_0 + \beta_1 X_{MFT} + \beta_2 X_{Watershed} + \beta_3 X_{TotPrecip} + \beta_4 X_{MFT}X_{Watershed}$	6	5.84	0.71	0.11
$Y_{Flow,3} \sim \beta_0 + \beta_1 X_{MFT} + \beta_2 X_{Watershed} + \beta_3 X_{TotPrecip}$	5	7.07	1.94	0.06
$Y_{Flow,4} \sim \beta_0 + \beta_1 X_{MFT} + \beta_2 X_{WTE} + \beta_3 X_{TotPrecip}$	5	7.08	1.96	0.06
$Y_{Flow,5} \sim \beta_0 + \beta_1 X_{MFT} + \beta_2 X_{WTE} + \beta_3 X_{TotPrecip} + \beta_4 X_{MFT}X_{WTE} + \beta_5 X_{AvgTemp}$	7	7.95	2.82	0.04
...				
$Y_{Flow} \sim \beta_0 + \beta_1 X_{SnowPeak}X_{MFT}X_{WTE}I_{Watershed} + \beta_2 X_{AvgTemp} + \beta_3 X_{TotPrecip}$	19	111.2	106.06	1.50E-24

is considered as a whole during the step-wise regression analysis, frost is not always the most important variable within each model.

Additionally, of the models tested with only a single predictor, the model with WTE had the most predictive power with a Δ AICc of 14.25 followed successively by the models with the catchment indicator (Δ AICc 15.25), average annual temperature (Δ AICc 25.11), total annual precipitation (Δ AICc 26.03), maximum frost thickness (Δ AICc 29.58), and finally peak snow depth (Δ AICc 31.38). Catchment indicator is high in these rankings

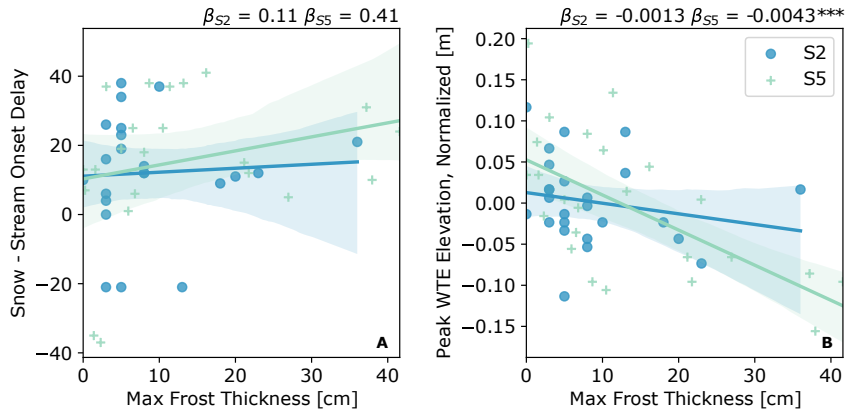


Figure 6. (A) Snow-Stream Onset Delay (Date of Stream Onset – Date of Peak Snow at MEF) as controlled by frost thickness. (B) Peak WTE, normalized by average WTE in each catchment, as a function of frost thickness. Beta values show the slopes for each relationship. Stars indicate the level of significance for each trend with *** denoting $p < 0.001$. Shaded areas indicate a 95% confidence interval.

395 because of the high correlation between catchment and average WTE. This result, and
 396 the results from the dominance analysis, suggest that frost is not the singular best in-
 397 dicator of streamflow, but is an important predictor in the context of other better stream-
 398 flow predictors like precipitation and WTE.

399 From the candidate models, it is important to note the interchangeability of WTE and
 400 catchment. Because the average WTE in S2 is lower than S5 (421m vs. 423m), WTE
 401 acts as a pseudo indicator variable for catchment but there is a slight dominance of WTE
 402 over catchment. For example the top two models in Table 2 are the same components
 403 other than the presence of either X_{WTE} variables in $Y_{Flow,1}$ or $I_{Watershed}$ in $Y_{Flow,2}$. Ad-
 404 ditionally, X_{WTE} has a slightly higher weight than $I_{Watershed}$ (Figure 5).

405 4 Discussion

406 We examined the interactions among climatological and hydrological drivers of stream-
 407 flow in snow-dominated catchments. Using long-term data from two headwater catch-
 408 ments at the Marcell Experimental Forest in northern Minnesota (S2 and S5), our anal-
 409 ysis showed that the annual streamflow decreased between 1995 and 2017, with S5 de-
 410 creasing at a faster rate than S2. In fact, S5 has shown little to no streamflow out of the
 411 peatland in the last 4 years of the record. These declining streamflow trends showed a
 412 small significant correlation ($p = 0.044$) with maximum annual snowpack (Figure S3)

413 but no significant correlation with various other climatic variables such as snowfall frac-
 414 tion (Figure 2b) and winter air temperature (Figure 2c). This lack of correlation sug-
 415 gests that the observed changes in streamflow must be considered in conjunction with
 416 other land surface drivers. One possible driver may be an increase in evapotranspiration
 417 caused by increases in surface energy and air temperature (Badger et al., 2021). How-
 418 ever, there is no correlation between air temperature and streamflow ($p > 0.5$), which
 419 means that while increasing evapotranspiration is still a possible cause, it likely is not
 420 the whole explanation (we could not perform direct analysis with respect to ET since
 421 direct measurements of ET are not available). Instead, we hypothesize that the decrease
 422 in streamflow is a result of the shifts in both hydrological connectivity within the wet-
 423 lands and how this connectivity regulates the streamflow generation processes. By ex-
 424 ploring the role of other climatological and hydrological drivers within the peatland catch-
 425 ments, our results illustrate the complex relationships between snow, water table eleva-
 426 tions, and streamflow, as well as the important role of soil frost in controlling these re-
 427 lations.

428 4.1 Hydrologic Connectivity

429 Our results show that within peatland catchments, there is a clear connection between
 430 WTE and streamflow, where the shift in peak WTE towards later in the spring induces
 431 a parallel shift in the first streamflow peak (Figure 3). This coupling between WTE and
 432 streamflow highlights the importance of hydrological connectivity within this system. Due
 433 to the elevated WTE in the spring compared to the rest of the year (Figure 1), this cou-
 434 pling also identifies the spring season as the most important part of the year for dictat-
 435 ing annual streamflow magnitude.

436 This hydrologic connectivity is also supported by the ranking analysis from Figure 4 which
 437 gives the sequence of events that lead to streamflow generation from the snowpack (Fig-
 438 ure 4). The first event in the ordering is the timing of the peak snowpack, indicating the
 439 beginning of the snow melt season. The second event is the timing of the lowest point
 440 in the WTE, the trough, which precedes recharge. There is a delay between these first
 441 two events potentially due to peatland storage, the refreezing of water into the snowpack
 442 as it melts (Heldmyer et al., 2021), ripening of the snowpack, or sublimation of snow back
 443 to the atmosphere. Once the water has begun reaching the peatland water table, the rank-
 444 ing scheme indicates that the water table then acts as a secondary storage system un-

445 til streamflow initiates. Streamflow onset is then initiated only after the WTE rises above
 446 a threshold relative to the outlet stream elevation (Figure 3a-b).

447 The date of frost disappearance was excluded from this ranking because of the low data
 448 resolution for frost depth, so the timing of soil frost in relation to water table recharge
 449 and streamflow onset is unknown. Past studies that have found no dependence between
 450 frost and streamflow timing have shown this is likely due to the frost thawing before recharge
 451 begins (Lindström et al., 2002), while other sites that have shown dependence between
 452 streamflow and soil frost have identified rapid streamflow response when precipitation
 453 is falling on frozen snow-free ground (Shanley & Chalmers, 1999). For our results to be
 454 put into context of these previous studies, higher frequency soil frost monitoring is needed.

455 4.2 Explanatory Power of Soil Frost

456 Although the role of soil frost disappearance timing remains uncertain, the stepwise mul-
 457 tiple regression model built to predict streamflow from both climatological and hydro-
 458 logical variables demonstrated a strong dependence on soil frost thickness. The five best
 459 performing models for streamflow each contains a combination of frost thickness, water
 460 table elevation, catchment, air temperature, and total annual precipitation. Peak snow-
 461 pack depth at the MEF is not selected as an important predictive variable in these top
 462 models, which was unexpected, given that past studies commonly use SWE to predict
 463 streamflow (Bayard et al., 2005; Ryberg et al., 2016). However, in our case, snow depth
 464 may not capture the same temporal variability in snow density as SWE, limiting the abil-
 465 ity to predict spring streamflow from snow depth.

466 Maximum frost thickness is the most highly weighted predictor variable when compared
 467 to all other possible predictors (with weight defined in Section 2.4). This result runs counter
 468 to the expectation that precipitation or snowpack, the more commonly used predictors
 469 for streamflow, would have the most weight. Total annual precipitation was the second
 470 highest weighted predictor followed by both WTE and catchment. However, it is impor-
 471 tant to note two things. First, when each of the predictor variables are used to predict
 472 streamflow on their own, maximum frost thickness has the second lowest explanatory
 473 power. Second, within the best model for streamflow, frost was only describing 12% of
 474 the total model variance. Similar to snowpack, soil frost is not present every year, and
 475 therefore should not be directly relied upon to solely predict streamflow. Instead, in ar-

476 eas where frost may appear, it should be considered as an important driver of stream-
 477 flow generation and a supporting predictor for streamflow amount.

478 This result is not unexpected, given the wealth of data showing the influence of soil frost
 479 on infiltration in both modelled soil columns (Zhao & Gray, 1999) and catchments on
 480 short time scales (<3 years, Shanley and Chalmers (1999)). Nevertheless, it reinforces
 481 the idea that frost is an important hydrologic factor even across long time scales. Ad-
 482 ditionally, while many of these analyses have looked at the effects of soil frost on infil-
 483 tration or streamflow (Ala-Aho et al., 2021; Bayard et al., 2005; Lindström et al., 2002),
 484 our results show *how* these effects extend to streamflow, lateral dynamics, and connec-
 485 tive fluxes across the catchment. Specifically, in areas where the season of frozen ground
 486 overlaps with the spring recharge season, as does in much of northern North America,
 487 soil frost is sometimes a dominant factor affecting both the timing and magnitude of recharge
 488 and streamflow in forested catchments. While it is unclear why soil frost seems to be par-
 489 ticularly influential in our studied catchments compared to forested catchments (Aho et
 490 al. 2021), one reason may be that the perched water table may make peatlands more sus-
 491 ceptible to higher frost contents in the upper ground layers. Higher frost content in the
 492 upper layers would cause more drastic restrictions in infiltration and a larger fraction
 493 of snowmelt being routed to streamflow.

494 **4.3 Applications to Water Balance Partitioning**

495 The presence of increased soil frost depth is generally known to either limit the infiltra-
 496 tion of water to the water table, making the recharge and baseflow processes slower and
 497 delaying streamflow initiation, or limit recharge altogether and cause rapid streamflow
 498 generation through overland flow (Ala-Aho et al., 2021; Fuss et al., 2016; Shanley & Chalmers,
 499 1999). These processes dictate the division of water between that which is available to
 500 plants for transpiration, and that which flows to streams. While the effects of different
 501 plant cover types, soil types, and snow cover distributions on water partitioning have been
 502 studied (Hammond et al., 2019), the coupled effects of soil frost on partitioning are still
 503 understudied. In this section we present several hypotheses and preliminary results to
 504 illustrate how frost could control snowmelt partitioning.

505 In the MEF catchments, the decoupled timing between snowpack melt and streamflow
 506 initiation implies that there may be an influence of frost on this partitioning in both S2

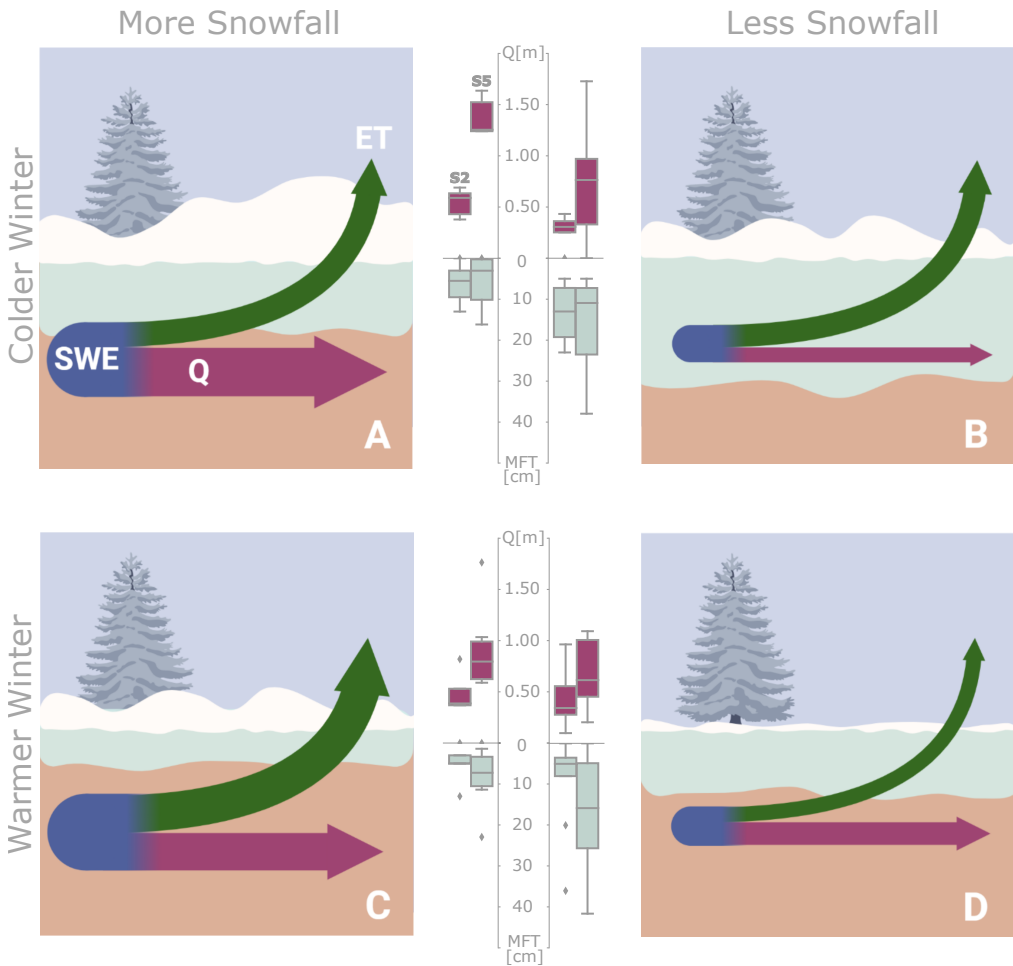


Figure 7. Conceptual diagram representing the effects that frost could have on the partitioning of precipitation into evapotranspiration and annual streamflow during and after snowmelt. Light blue shading represents frost depth. Relative magnitude of SWE due to snowfall is shown in dark blue. SWE splits into diverging arrows to show the relative partition between evapotranspiration (dark green) and streamflow (purple) respectively. The center column shows frost depth data (light blue) and total annual streamflow data (purple) from the MEF partitioned into each of the four scenarios. Deep vertical drainage, though known to occur in S2 and S5 (Verry et al., 2011), is not depicted for simplicity.

507 and S5. Figure 7 shows a depiction of how different snowfall and winter temperature sce-
 508 narios may dictate (i) the depth of the frost layer and (ii) the partitioning of SWE for
 509 spring streamflow and evapotranspiration. In each proposed scenario, data from the S2
 510 and S5 catchments (1995–2020) have been divided into each of four winter temperature
 511 and snowfall scenarios. Years with winter temperatures above the average are consid-
 512 ered 'warmer winter' and years with snowfall totals above the average are considered 'more
 513 snowfall' (and vice versa). Scenario A shows the baseline conditions at the MEF where
 514 there is more snowfall and colder winter temperatures compared to future projected con-
 515 ditions. In this scenario, a large snowpack and colder temperatures result in a lower max-
 516 imum frost thickness compared to a deeper frost depth in scenario B (see light blue box-
 517 plots in upper row), where there is little snow and less insulation, or the thin frost layer
 518 in C where there are warmer temperatures. Because of the deeper snowpacks, scenar-
 519 ios A and C will have more water available than in scenarios B and D respectively (Fig-
 520 ure 7, dark blue areas in the arrows).

521 Snow water equivalent represents the amount of water that is available to recharge soil
 522 storage or runoff to spring streamflow, thus less SWE can result in a reduction in over-
 523 all streamflow water availability (Barnett et al. (2005) ; Figure 7A to B, or C to D, pur-
 524 ple arrows and boxplots). Additionally, the depth of soil frost may control the partition-
 525 ing of SWE over two steps: first, by controlling the amount of soil water availability in
 526 early spring, and then, the amount of soil water taken up by evapotranspiration in the
 527 late spring. In the first stage, the presence of frost limits early snowmelt infiltration and
 528 enhances surface runoff to streamflow, but we hypothesize that a reduction in vertical
 529 drainage may also increase saturation in the top part of the peat soil column. In the sec-
 530 ond stage, transpiration is assumed to start only after the ground has thawed and af-
 531 ter leaf out (Mellander et al., 2006). Here, because the melting of the frost layer depends
 532 on the insulation effects of snow, snow also plays a role in determining the timing of trans-
 533piration onset. Therefore, the magnitude of spring evapotranspiration will depend both
 534 on the timing of soil frost disappearance and the amount of soil frost. For example, in
 535 scenario A, there is a large amount of water available in the snowpack, and because of
 536 the deep frost layer coupled with the deep snowpack, more of the water is lost to over-
 537 land flow due to inhibited infiltration and delayed transpiration onset (therefore Q in A
 538 $> Q$ in C and ET in A $< ET$ in C despite the same snowfall inputs). However, compar-
 539 ing scenario B to A, there is a thicker frost layer, as confirmed by the MEF data, but

540 a larger fraction of the available water is directed towards evapotranspiration because
 541 the frost layer melts out more quickly due to the small snowpack, leaving more time for
 542 transpiration in the spring. This is reflected in the data from S2 and S5 which respec-
 543 tively show a lower amount of annual streamflow in scenario B compared to scenario A.
 544 There is also a lot more variation in the data during the years with less snowfall, likely
 545 due a patchy snow cover.

546 This redistribution of soil water storage toward earlier spring evapotranspiration with
 547 deep frost and little snowfall could lead to overall increases in the evaporative fraction
 548 of meltwater inputs. We can see that if winter temperatures increase and snowfall rates
 549 stay constant (A → C), there may actually be overall increase in evapotranspiration
 550 at the expense of streamflow. If winter temperatures remain constant but snowfall de-
 551 creases (A → B) the rates of evapotranspiration may remain relatively constant despite
 552 the decrease in water availability, because of the shift in partitioning due to frost. If there
 553 are simultaneous increases in temperature and decreases in snowfall (A → D) the par-
 554 tition remains relatively the same. Accordingly, we could observe decreases in both evap-
 555 otranspiration rates and overland runoff. Therefore, it is important to consider the in-
 556 teractions of snow, frost, and water table dynamics, when determining SWE partition-
 557 ing in headwater catchments like the MEF.

558 5 Conclusions

559 Our results demonstrated the hydrologic connectivity between the snowpack, water ta-
 560 ble, frost, and streamflow during the winter-spring transition, and highlights the impor-
 561 tance of frost in streamflow generation in peatlands. This research shows that in the con-
 562 text of catchment management, it is important to monitor the snow pack and the frost
 563 layer. Together, the interactions between snow and frost give a more holistic understand-
 564 ing of streamflow generation. These interactions need to be properly accounted for in
 565 hydrological and land surface models, so that we can improve our abilities to predict long-
 566 term catchment response to environmental change and improve water management.

567 6 Open Research

568 All data used in this paper is accessible online at the following locations:

- **MEF precipitation:** Sebestyen, S.D., D.T. Roman, J.M. Burdick, N.K. Lany, R.L. Kyllander, A.E. Elling, E.S. Verry, and R.K. Kolka. 2021. Marcell Experimental Forest daily precipitation, 1961 - ongoing ver 2. Environmental Data Initiative. <https://doi.org/10.6073/pasta/61c7154b78f521841ff8e25fc6db9987>
- **MEF soil frost:** Sebestyen, S.D., E.S. Verry, A.E. Elling, R.L. Kyllander, D.T. Roman, J.M. Burdick, N.K. Lany, and R.K. Kolka. 2020. Marcell Experimental Forest biweekly bog frost depth, 1985 - ongoing ver 1. Environmental Data Initiative. <https://doi.org/10.6073/pasta/0f184840135054ab017c8aad6496c353>
- **MEF snow and SWE:** Sebestyen, S.D., J.M. Burdick, D.T. Roman, N.K. Lany, R.L. Kyllander, A.E. Elling, E.S. Verry, and R.K. Kolka. 2021. Marcell Experimental Forest biweekly snow depth, frost depth, and snow water equivalent, 1962 - ongoing ver 2. Environmental Data Initiative.
<https://doi.org/10.6073/pasta/2ff0a9c2cce5a130b7b51fefe7ff38c6>
- **MN DNR snow and SWE:** Courtesy of the Minnesota Department of Natural Resources Grand Rapids Forestry Lab - Station 213303. Data available here: <https://www.dnr.state.mn.us/climate/historical/daily-data.html>
- **MEF streamflow:** Verry, Elon S.; Elling, Arthur E.; Sebestyen, Stephen D.; Kolka, Randall K.; Kyllander, Richard. 2018. Marcell Experimental Forest daily streamflow data. Fort Collins, CO: Forest Service Research Data Archive.
<https://doi.org/10.2737/RDS-2018-0009>
- **MEF WTE:** Sebestyen, S.D., J.M. Burdick, D.T. Roman, N.K. Lany, R.L. Kyllander, A.E. Elling, E.S. Verry, and R.K. Kolka. 2021. Marcell Experimental Forest daily peatland water table elevation, 1961 - ongoing ver 2. Environmental Data Initiative. <https://doi.org/10.6073/pasta/2a75c323256252a763e9343f0df7b6af>

593 **Acknowledgments**

594 M.J. and X.F. were supported by the Department of Energy Environmental System Science grant DE-SC0019036. The long-term monitoring at the MEF and the contributions
595 of S.D.S are funded by the Northern Research Station of the USDA Forest Service.
596

597 **References**

598 Ala-Aho, P., Autio, A., Bhattacharjee, J., Isokangas, E., Kujala, K., Marttila, H.,
 599 ... Kløve, B. (2021). What conditions favor the influence of seasonally frozen
 600 ground on hydrological partitioning? A systematic review. *Environ. Res. Lett.*,
 601 *16*, 43008. Retrieved from <https://doi.org/10.1088/1748-9326/abe82c>
 602 doi: 10.1088/1748-9326/abe82c

603 Alexander, R. B., Boyer, E. W., Smith, R. A., Schwarz, G. E., & Moore, R. B.
 604 (2007). The Role of Headwater Streams in Downstream Water Qual-
 605 ity. *Journal of the American Water Resources Association (JAWRA)*.
 606 *J*, *43*(1), 41–59. Retrieved from www.blackwell-synergy.com doi:
 607 10.1111/j.1752-1688.2007.00005.x

608 Aygün, O., Kinnard, C., & Campeau, S. (2019, 10). Impacts of climate change
 609 on the hydrology of northern midlatitude cold regions:. <https://doi->
 610 org.ezp1.lib.umn.edu/10.1177/0309133319878123, *44*(3), 338–375. Retrieved
 611 from <https://journals-sagepub-com.ezp1.lib.umn.edu/doi/10.1177/0309133319878123> doi: 10.1177/0309133319878123

613 Badger, A. M., Bjarke, N., Molotch, N. P., & Livneh, B. (2021, 9). The sensitivity
 614 of runoff generation to spatial snowpack uniformity in an alpine watershed:
 615 Green Lakes Valley, Niwot Ridge Long-Term Ecological Research station.
 616 *Hydrological Processes*, *35*(9). Retrieved from <https://doi.org/10.1002/hyp.14331>
 617 doi: 10.1002/hyp.14331

619 Barnett, T. P., Adam, J. C., & Lettenmaier, D. P. (2005, 11). Potential impacts of
 620 a warming climate on water availability in snow-dominated regions. *Nature*,
 621 *438*(7066), 303–309. Retrieved from <http://www.nature.com/articles/nature04141> doi: 10.1038/nature04141

623 Bayard, D., Stähli, M., Parriaux, A., & Flühler, H. (2005, 7). The influence of
 624 seasonally frozen soil on the snowmelt runoff at two Alpine sites in south-
 625 ern Switzerland. *Journal of Hydrology*, *309*(1-4), 66–84. Retrieved from
 626 <https://linkinghub.elsevier.com/retrieve/pii/S0022169404005633>
 627 doi: 10.1016/j.jhydrol.2004.11.012

628 Berghuijs, W. R., Woods, R. A., & Hrachowitz, M. (2014). A precipitation shift
 629 from snow towards rain leads to a decrease in streamflow. *Nature Climate*

663 Mediated by Seasonal Hydrologic Dynamics. *Geophysical Research Letters*,
 664 47(17), 1–9. doi: 10.1029/2020GL088875

665 Ford, C. M., Kendall, A. D., & Hyndman, D. W. (2020). Effects of shifting
 666 snowmelt regimes on the hydrology of non-alpine temperate landscapes. *Jour-*
 667 *nal of Hydrology*, 590(March), 125517. Retrieved from <https://doi.org/10.1016/j.jhydrol.2020.125517> doi: 10.1016/j.jhydrol.2020.125517

668 Foster, L. M., Bearup, L. A., Molotch, N. P., Brooks, P. D., & Maxwell, R. M.
 669 (2016). Energy budget increases reduce mean streamflow more than snow-
 670 rain transitions: using integrated modeling to isolate climate change im-
 671 pacts on Rocky Mountain hydrology. *Environ. Res. Lett.*, 11, 44015. doi:
 672 10.1088/1748-9326/11/4/044015

673 Fuss, C. B., Driscoll, C. T., Green, M. B., & Groffman, P. M. (2016, 11). Hy-
 674 drologic flowpaths during snowmelt in forested headwater catchments un-
 675 der differing winter climatic and soil frost regimes. *Hydrological Pro-*
 676 *cesses*, 30(24), 4617–4632. Retrieved from <https://onlinelibrary-wiley-com.ezp3.lib.umn.edu/doi/full/10.1002/hyp.10956> doi:
 677 10.1002/hyp.10956

678 Golden, H. E., Sander, H. A., Lane, C. R., Zhao, C., Price, K., D'Amico, E., &
 679 Christensen, J. R. (2016, 1). Relative effects of geographically isolated wet-
 680 lands on streamflow: a watershed-scale analysis. *Ecohydrology*, 9(1), 21–38.
 681 Retrieved from <https://onlinelibrary.wiley.com/doi/10.1002/eco.1608> doi: 10.1002/eco.1608

682 Gorham, E. (1991). Northern Peatlands : Role in the Carbon Cycle and Probable
 683 Responses to Climatic Warming. *Ecological Applications*, 1(2), 182–195.

684 Hammond, J. C., Harpold, A. A., Weiss, S., & Kampf, S. K. (2019). Partition-
 685 ing snowmelt and rainfall in the critical zone: Effects of climate type and
 686 soil properties. *Hydrology and Earth System Sciences*, 23(9), 3553–3570.
 687 Retrieved from <https://doi.org/10.5194/hess-23-3553-2019> doi:
 688 10.5194/hess-23-3553-2019

689 Heldmyer, A., Livneh, B., Molotch, N. P., & Rajagopalan, B. (2021). Investigat-

696 ing the Relationship Between Peak Snow-Water Equivalent and Snow Timing
697 Indices in the Western United States and Alaska. *Water Resources Research*.
698 doi: 10.1029/2020WR029395

699 Hodgkins, G. A., & Dudley, R. W. (2006). Changes in the timing of winter-spring
700 streamflows in eastern North America, 1913-2002. *Geophys. Res. Lett.*, *33*,
701 6402. doi: 10.1029/2005GL025593

702 Jyrkama, M. I., & Sykes, J. F. (2007). The impact of climate change on spatially
703 varying groundwater recharge in the grand river watershed (Ontario). *Journal*
704 *of Hydrology*, *338*(3-4), 237-250. doi: 10.1016/j.jhydrol.2007.02.036

705 Kane, D. L., & Stein, J. (1983, 12). Water movement into seasonally frozen
706 soils. *Water Resources Research*, *19*(6), 1547-1557. Retrieved from
707 <https://agupubs-onlinelibrary-wiley-com.ezp3.lib.umn.edu/doi/full/10.1029/WR019i006p01547>
708 <https://agupubs-onlinelibrary-wiley-com.ezp3.lib.umn.edu/doi/abs/10.1029/WR019i006p01547>
709 <https://agupubs-onlinelibrary-wiley-com.ezp3.lib.umn.edu/doi/10.1029/WR019i0> doi:
710 10.1029/WR019i006p01547

711

712 Leibowitz, S. G., & Vining, K. C. (2003). TEMPORAL CONNECTIVITY IN A
713 PRAIRIE POTHOLE COMPLEX. *WETLANDS*, *23*(1), 13-25.

714 Leuthold, S. J., Ewing, S. A., Payn, R. A., Miller, F. R., & Custer, S. G. (2021,
715 2). Seasonal connections between meteoric water and streamflow generation
716 along a mountain headwater stream. *Hydrological Processes*, *35*(2). Retrieved
717 from <https://onlinelibrary.wiley.com/doi/10.1002/hyp.14029> doi:
718 10.1002/hyp.14029

719 Lindström, G., Bishop, K., & Löfvenius, M. O. (2002, 12). Soil frost and runoff at
720 Svartberget, northern Sweden - Measurements and model analysis. *Hydrological*
721 *Processes*, *16*(17), 3379-3392. doi: 10.1002/hyp.1106

722 McDonnell, J. J., Spence, C., Karran, D. J., van Meerveld, H. J. I., & Harman,
723 C. J. (2021, 5). Fill-and-Spill: A Process Description of Runoff Generation
724 at the Scale of the Beholder. *Water Resources Research*, *57*(5). Retrieved
725 from <https://onlinelibrary.wiley.com/doi/10.1029/2020WR027514> doi:
726 10.1029/2020WR027514

727 Mellander, P.-E., Stähli, M., Gustafsson, D., & Bishop, K. (2006, 6). Modelling
728 the effect of low soil temperatures on transpiration by Scots pine. *Hydrolog-*

729 *ical Processes*, 20(9), 1929–1944. Retrieved from www.interscience.wiley.com/https://onlinelibrary.wiley.com/doi/10.1002/hyp.6045 doi:
730 [10.1002/hyp.6045](https://doi.org/10.1002/hyp.6045)

731

732 Murray, K., & Conner, M. M. (2009, 2). Methods to quantify variable importance:
733 implications for the analysis of noisy ecological data. *Ecology*, 90(2), 348–355.
734 Retrieved from <http://doi.wiley.com/10.1890/07-1929.1> doi: 10.1890/07-1929.1

735

736 Musselman, K. N., Addor, N., Vano, J. A., & Molotch, N. P. (2021). Winter melt
737 trends portend widespread declines in snow water resources. *Nature Climate
738 Change*. doi: 10.1038/s41558-021-01014-9

739

740 Pringle, C. (2003). What is hydrologic connectivity and why is it ecologically im-
741 portant? *Hydrol. Process Invited Commentary*, 17, 2685–2689. Retrieved from
742 www.interscience.wiley.com doi: 10.1002/hyp.5145

743

744 Richardson, M. C., Mitchell, C. P., Branfireun, B. A., & Kolka, R. K. (2010, 9).
745 Analysis of airborne LiDAR surveys to quantify the characteristic morpholo-
746 gies of northern forested wetlands. *Journal of Geophysical Research: Bioge-
747 osciences*, 115(3). doi: 10.1029/2009JG000972

748

749 Ryberg, K. R., Akyüz, F. A., Wiche, G. J., & Lin, W. (2016, 4). Changes in
750 seasonality and timing of peak streamflow in snow and semi-arid climates
751 of the north-central United States, 1910–2012. *Hydrological Processes*,
752 30(8), 1208–1218. Retrieved from <http://nwis.waterdata.usgs.gov/usa/https://onlinelibrary.wiley.com/doi/10.1002/hyp.10693> doi:
753 [10.1002/hyp.10693](https://doi.org/10.1002/hyp.10693)

754

755 Schneider, D., & Molotch, N. P. (2016). Real-time estimation of snow water
756 equivalent in the Upper Colorado River Basin using MODIS-based SWE
757 Reconstructions and SNOTEL data. *Water Resources Research*, 52(10),
758 7892–7910. Retrieved from <http://www.wcc.nrcs.usda.gov/snow/> doi:
759 [10.1002/2016WR019067](https://doi.org/10.1002/2016WR019067)

760

761 Sebestyen, S., Burdick, J. M., Roman, D. T., Lany, N. K., Kylander, R. L.,
762 Elling, A., ... Kolka, R. K. (2021). *Marcell Experimental Forest daily
763 peatland water table elevation, 1961 - ongoing, 2 ed.* (Tech. Rep.). USDA
764 Forest Service, Environmental Data Initiative. Retrieved from <https://doi.org/10.6073/pasta/2a75c323256252a763e9343f0df7b6af> doi:
765

762 <https://doi.org/10.6073/pasta/2a75c323256252a763e9343f0df7b6af>

763 Sebestyen, S., Dorrance, C., Olson, D., Verry, E., Kolka, R., Elling, A., & Kyl-
764 lander, R. (2011, 2). Long-Term Monitoring Sites and Trends at the Mar-
765 cell Experimental Forest. In *Peatland biogeochemistry and watershed hy-
766 drology at the marcell experimental forest* (pp. 15–71). CRC Press. Re-
767 trieved from <http://www.crcnetbase.com/doi/10.1201/b10708-3> doi:
768 10.1201/b10708-3

769 Sebestyen, S., Lany, N. K., Roman, D. T., Burdick, J. M., Kyllander, R. L., Verry,
770 E. S., & Kolka, R. K. (2021, 3). Hydrological and meteorological data from
771 research catchments at the Marcell Experimental Forest, Minnesota, USA.
772 *Hydrological Processes*, 35(3). Retrieved from <https://doi.org/10.1002/hyp.14092>
773 doi: 10.1002/hyp.14092

774 Shanley, J. B., & Chalmers, A. (1999). The effect of frozen soil on snowmelt runoff
775 at Sleepers River, Vermont. *Hydrological Processes*, 13, 1843–1857.

776 Trujillo, E., & Molotch, N. P. (2014). Snowpack regimes of the Western
777 United States. *Water Resources Research*(50), 5375–5377. doi: 10.1002/
778 2013WR014979.Reply

780 Verry, E. S., Brooks, K. N., Nichols, D. S., Ferris, D. R., & Sebestyen, S. D. (2011,
781 2). Watershed Hydrology. In *Peatland biogeochemistry and watershed hydrol-
782 ogy at the marcell experimental forest* (pp. 193–212). CRC Press. doi: 10.1201/
783 b10708-8

784 Verry, E. S., Elling, A., Sebestyen, S., Kolka, R. K., & Kyllander, R. L. (2018). *Mar-
785 cell Experimental Forest daily streamflow data, 1 ed.* (Tech. Rep.). Fort Collins,
786 Co.: Forest Service Research Data Archive. Retrieved from <https://doi.org/10.2737/RDS-2018-0009> doi: <https://doi.org/10.2737/RDS-2018-0009>

788 Virtanen, P., Gommers, R., Oliphant, T. E., Haberland, M., Reddy, T., Cournapeau,
789 D., . . . Contributors, S. . (2020). SciPy 1.0: Fundamental Algorithms for
790 Scientific Computing in Python. *Nature Methods*, 17, 261–272. Retrieved from
791 <https://rdcu.be/b08Wh> doi: 10.1038/s41592-019-0686-2

792 Winter, T. C., & LaBaugh, J. W. (2003). Hydrologic considerations in defining
793 isolated wetlands. *Wetlands*, 23(3), 532–540. doi: 10.1672/0277-5212(2003)
794 023[0532:HCIDIW]2.0.CO;2

795 Zhao, L., & Gray, D. M. (1999). Estimating snowmelt infiltration into frozen soils.
796 *Hydrological Processes*, 13, 1827–1842.